

7-2023

Mapping California Rice Using Optical and SAR Data Fusion with Phenological Features in Google Earth Engine

Li Wenzhao

Chapman University, li276@mail.chapman.edu

Hesham el-Askary

Chapman University, elaskary@chapman.edu

Daniele C. Struppa

Chapman University, struppa@chapman.edu

Follow this and additional works at: https://digitalcommons.chapman.edu/scs_articles



Part of the [Agriculture Commons](#), and the [Remote Sensing Commons](#)

Recommended Citation

W. Li, H. El-Askary and D. C. Struppa, "Mapping California Rice Using Optical and SAR Data Fusion with Phenological Features in Google Earth Engine," *IGARSS 2023 - 2023 IEEE International Geoscience and Remote Sensing Symposium*, Pasadena, CA, USA, 2023, pp. 5619-5622, <https://doi.org/10.1109/IGARSS52108.2023.10281418>.

This Conference Proceeding is brought to you for free and open access by the Science and Technology Faculty Articles and Research at Chapman University Digital Commons. It has been accepted for inclusion in Mathematics, Physics, and Computer Science Faculty Articles and Research by an authorized administrator of Chapman University Digital Commons. For more information, please contact laughtin@chapman.edu.

Mapping California Rice Using Optical and SAR Data Fusion with Phenological Features in Google Earth Engine

Comments

This is a pre-copy-editing, author-produced PDF of an article accepted for publication in *IGARSS 2023 - 2023 IEEE International Geoscience and Remote Sensing Symposium*. This article may not exactly replicate the final published version. The definitive publisher-authenticated version is available online at <https://doi.org/10.1109/IGARSS52108.2023.10281418>.

Copyright

© 2023 IEEE. Personal use of this material is permitted. Permission from IEEE must be obtained for all other uses, in any current or future media, including reprinting/republishing this material for advertising or promotional purposes, creating new collective works, for resale or redistribution to servers or lists, or reuse of any copyrighted component of this work in other works.

MAPPING CALIFORNIA RICE USING OPTICAL AND SAR DATA FUSION WITH PHENOLOGICAL FEATURES IN GOOGLE EARTH ENGINE

Wenzhao Li, Hesham El-Askary, Daniele C. Struppa

Schmid College of Science and Technology, Chapman University, Orange, CA, 92866

ABSTRACT

California, known for its diverse agriculture, is also a major producer of rice, especially in its northern regions in Sacramento River Valley. Traditional methods, predominantly reliant on optical-based satellite imagery, encounter limitations due to atmospheric interference and sensor resolution. The ability of Synthetic Aperture Radar (SAR) to penetrate atmospheric distortions and exhibit high sensitivity to vegetation structure presents a distinct advantage over optical-based methods. Utilizing Optical and SAR data fusion, this study advances the enhanced pixel-based phenological feature composite (Eppf) method using SVM classification algorithm, which can track phenological changes and patterns, providing valuable insights for agricultural planning and management. We demonstrate that Radar Vegetation Index (RVI) derived from SAR data, offers an improved alternative for identifying and mapping rice fields with enhanced accuracy. Subsequent research will focus on enhancing the suggested approach and investigating its relevance and adaptability to different types of crops.

Index Terms— Rice Mapping, Data Fusion, Sacramento River Valley, Radar Vegetation Index, Google Earth Engine

1. INTRODUCTION

The Sacramento River Valley (SRV) is the largest rice-growing region in California. The recent drought and water shortage in 2022 had made its rice grower plant less grain to be the smallest since 1977 [1]. Mapping and monitoring rice fields is essential for efficient resource allocation, aiding in sustainable agricultural practices by optimizing water, fertilizer, and pesticide usage. The detailed data obtained supports informed decision-making regarding planting schedules, irrigation, and harvesting, thereby enhancing yield and contributing to food security. Additionally, this process enables early detection of potential issues like diseases or pests, allowing for prompt interventions and minimizing crop losses. Remote sensing (RS) technology has been harnessed to comprehensively monitor vegetation growth patterns, offering extensive spatial coverage and temporal flexibility, surpassing the limitations of traditional field surveys [2]–[7]. This approach allows data collection over large geographical areas and at various time intervals, facilitating continuous crop monitoring and capturing

integral changes in growth stages and irrigation events. The recent method advances also introduced RS phenological features to separate of rice with others (e.g., dry and wetland vegetation), such as combined Consideration of Vegetation phenology and Surface water variations (CCVS) method [8], and enhanced pixel-based phenological feature composite (Eppf) method [9], where both chose one or more RS vegetation indices for different phenological periods (e.g., transplanting, tillering), achieving overall higher accuracies than many other un-phenological approaches. However, these existing methods used only a single optical sensor (MODIS or Sentinel-2), and the Eppf method had to combine three years of data (2017-2019) to save enough sampling images for phenological features, thus limiting their capacity for annual monitoring and yield estimation. Meanwhile, the unique capability of Synthetic Aperture Radar (SAR) to overcome atmospheric interferences and demonstrate heightened sensitivity to the structure of vegetation and land surface, offering a marked edge over techniques reliant on optical data on various applications [10]. This study is fundamentally designed to integrate two distinct types of remote sensing data: optical data, drawn from the Sentinel-2 and Landsat-8 satellites, and SAR data, sourced from the Sentinel-1 satellite. The objective of this integration is to maximize the potential of the phenological remote sensing approach for annual rice mapping, particularly in SRV region, where accurate and timely rice mapping can significantly contribute to resource management and yield optimization.

2. METHODOLOGY

As shown in the workflow chart in Figure 1, this study can be divided into three stages: (1) Data preprocessing, (2) Phenology analysis, and (3) Rice mapping. For the Data preprocessing stage, the Sentinel-2 and Landsat-8 imagery are processed by filtering images with cloud percentage > 70%. Sentinel-1 imagery is also processed to filter the speckle noise, which is considered strictly impact mapping accuracy [11]. Besides, the Landsat-8 sensor is adjusted to be harmonized with Sentinel-2 using parameters in [12] for data merging. Time series of optical indices (EVI2, BSI, LSWI, NDVI, and PSRI) and Sentinel-1 specialized RVI index are produced (the rationale of indices choice can be found in [8], [9], [13]). For the Phenology analysis stage, the CCSV method employs a growth curve from the indices and ratio of change (RCLE) for later use. For the Eppf method,

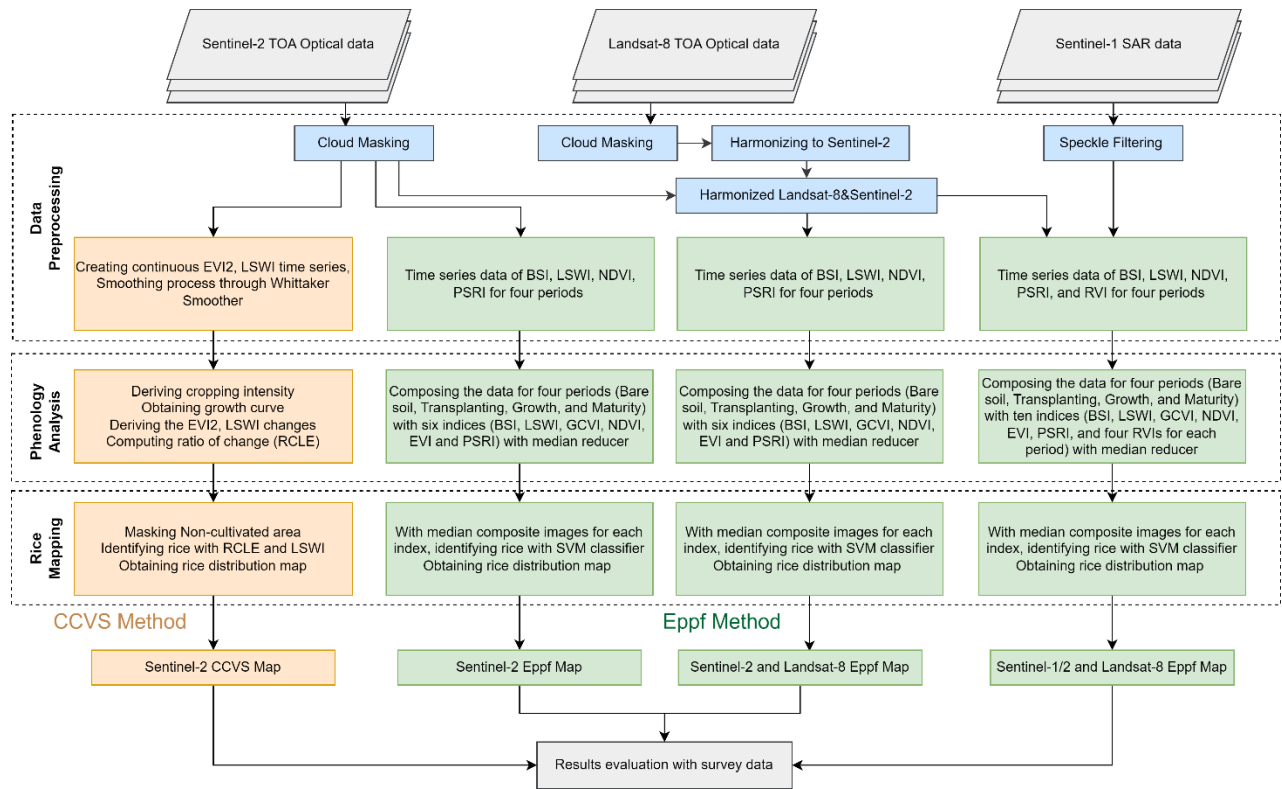


Fig. 1 Workflow chart of the study

the indices are composed for each predefined period (Bare soil, Transplanting, Growth, and Maturity) [9] in 2018 with median reducer. GCVI and EVI are additionally introduced. For the Rice mapping stage, CCSV identifies rice with RCLC and LSWI with the threshold values. For Eppf, an SVM classifier is used to obtain a rice distribution map. The maps will be evaluated with the 2018 survey data [8]. All these three stages are deployed fully on Google Earth Engine to achieve high efficiency, also showing great potential for further utilization anywhere worldwide.

The performance of the model was evaluated by visual comparison with the California statewide crop mapping data (<https://data.cnra.ca.gov/dataset/statewide-crop-mapping>) [14], and quantitatively (~ 400000 sampling observations over the study area) using a range of accuracy assessment metrics, including overall accuracy, Kappa coefficient, sensitivity, and specificity, and the results were compared with ground truth survey data. Overall accuracy provides a holistic view of the model's performance by measuring the proportion of correctly predicted observations to the total observations. The Kappa coefficient, on the other hand, offers an assessment of the model's accuracy while accounting for the accuracy obtained by chance, thereby presenting a more robust measure of reliability. Sensitivity (also known as true positive rate) quantifies the model's ability to correctly identify positive instances, in this case, rice fields, while specificity (true negative rate) gauges the model's proficiency in correctly identifying negative

instances, namely non-rice fields. Together, these metrics provide a comprehensive view of the model's performance, allowing us to ascertain its effectiveness in differentiating rice fields from other types of land cover as compared to the survey data.

3. RESULTS AND DISCUSSION

Figure 2 presents a comparative view of the mapping outcomes from different methodologies, namely, the CCSV (Fig. 2a), the Eppf utilizing only Sentinel-2 (Fig. 2b), the Eppf employing harmonized Sentinel-2 and Landsat-8 data (Fig. 2c), and the Eppf integrating Sentinel-1/2 and Landsat-8 data (Fig. 2d). These results are juxtaposed against the 2018 rice survey data [14] for a comprehensive evaluation (Fig. 2e).

The CCSV result delineates a less precise mapping compared to all Eppf outcomes, with extraneous pixelated regions being erroneously identified as rice fields, as denoted by the black squared regions in Fig. 2a. This discrepancy could be attributed to the inherent design of the original CCSV, which was tailored for MODIS daily data, whereas the Sentinel-2 data utilized in this study has a longer revisit time of at least ten days. Nevertheless, it's worth noting that the CCSV still manages to capture a generally accurate depiction of rice distribution, negating the need for sampling that is typically necessitated in the Eppf approach.

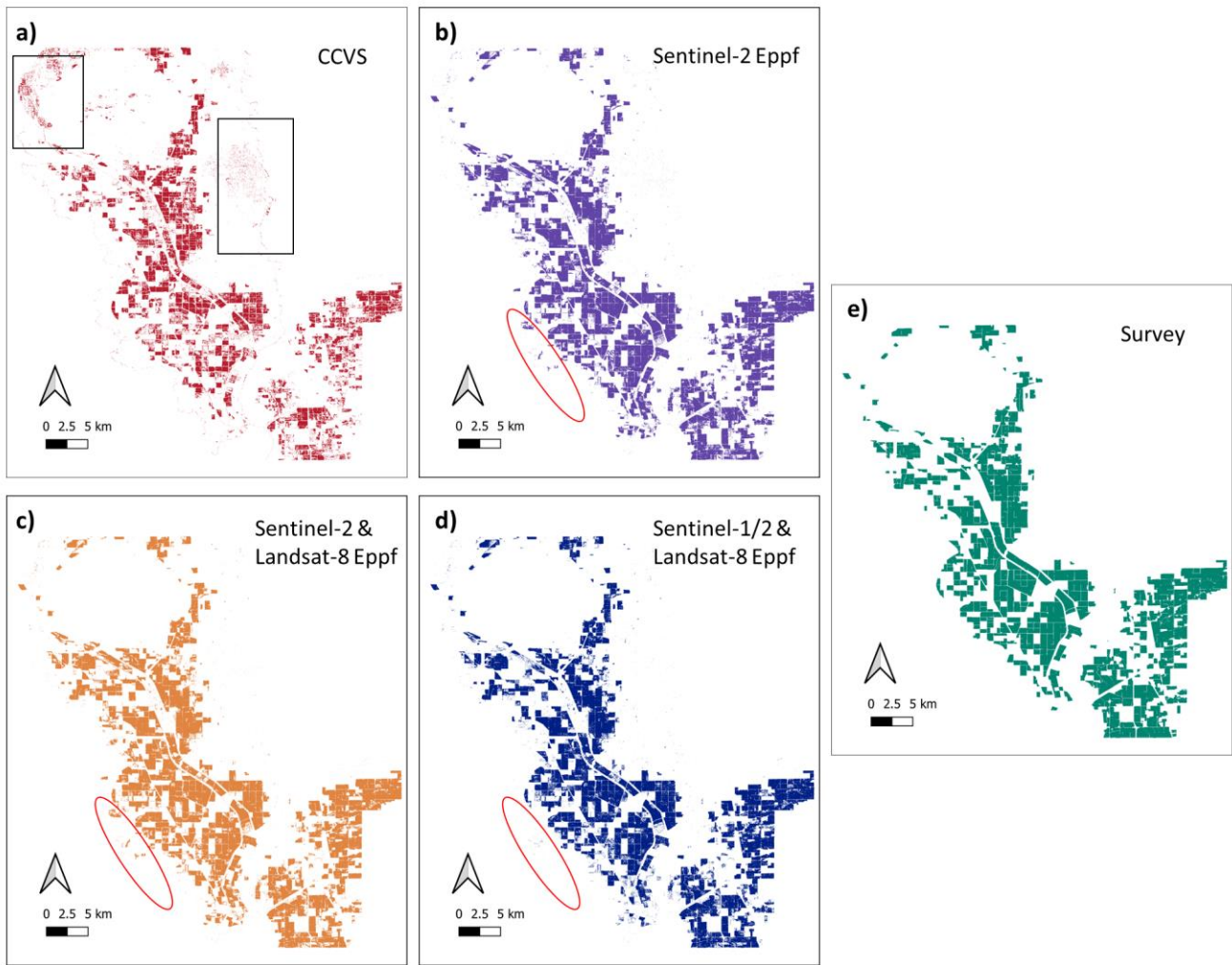


Fig. 2 Rice distribution map from a) CCVS, b-d) Eppf methods, and e) Survey data

When comparing Fig. 2b and Fig. 2c, no significant disparities can be discerned in relation to the distribution of rice fields, with the red circled region being inaccurately marked as rice in both instances. This observation suggests that the incorporation of additional images from Landsat-8 does not markedly alter the median indices values for each period, resulting in similar SVM classifiers as employed in Fig. 2b, which may be due to the simplified parameter based fusion method applied here [12]. Thus, the incorporation of Landsat-8 imagery seems to have a minimal effect on the resultant classification of rice fields in this case. Furthermore, a noticeable enhancement in the mapping results is observed with the inclusion of the RVI index derived from Sentinel-1 SAR images (Fig. 2d). This demonstrates the efficacy of integrating SAR data with optical imagery for rice field mapping. Specifically, the area demarcated by the red circle, which was previously mismarked in the optical-only imagery, is now correctly

identified as having no rice coverage, aligning more accurately with the survey map.

Table 1 shows similar results as shown in Figure 2, that the model with Sentinel-1 SAR contribution shows higher overall accuracy and Kappa values. This would suggest that the model is highly reliable in correctly identifying and mapping rice fields, and that its accuracy is not simply due to chance. However, for the same rice mapping model presented in Table 1, relatively low sensitivity but high specificity values would mean that the model sometimes fails to correctly identify areas that are actually rice fields, but it is very good at correctly identifying areas that are not rice fields. This could result in underestimation of the total rice cultivation area due to the results presented are pixel-based according to satellite imagery. Transitioning from pixel-based to object-based results via a further segmentation process can enhance the accuracy of crop mapping, particularly in addressing underestimation issues. This underestimation often arises from mixed pixels, which

contain both rice and non-rice elements, being misclassified as non-rice. Aggregating these mixed pixels into larger areas allows for better recognition of rice presence, reducing underestimation. Ultimately, object-based results offer a more realistic representation of agricultural landscapes, underscoring the value of this segmentation process in crop mapping models.

Table 1 Accuracy assessment of different models

| | Accuracy | Kappa | Sensitivity | Specificity |
|---------------|----------|-------|-------------|-------------|
| CCVS | 0.86 | 0.60 | 0.54 | 0.98 |
| Eppf_S2 | 0.93 | 0.82 | 0.85 | 0.96 |
| Eppf_S2_LS8 | 0.93 | 0.82 | 0.86 | 0.96 |
| Eppf_S1/2_LS8 | 0.94 | 0.86 | 0.84 | 0.98 |

The study shows the fusion of optical and SAR images can improve the rice mapping accuracy with the phenological feature in California rice fields, which open up new avenues for agricultural monitoring and resource management using advanced remote sensing methods, underscoring the potential for further improvements and applications. Future work will delve into refining the proposed methodology and exploring its applicability to other crop types by: 1) using customized Harmonized Landsat Sentinel-2 (HLS) product for optical imagery fusion; 2) improving the sampling process with the automatic and layered approach [15]; 3) optimizing and localizing the phenology periods for California rice growth; 4) implementing image segmentation to convert the pixel-based to object-based maps; 5) using other advanced machine learning algorithms (e.g., deep learning).

4. REFERENCES

- [1] "U.S. rice imports in 2022/23 are projected at an all-time high." <http://www.ers.usda.gov/data-products/chart-gallery/gallery/chart-detail/?chartId=104751> (accessed Jan. 20, 2023).
- [2] J. Dong and X. Xiao, "Evolution of regional to global paddy rice mapping methods: A review," *ISPRS J. Photogramm. Remote Sens.*, vol. 119, pp. 214–227, Sep. 2016, doi: 10.1016/j.isprsjprs.2016.05.010.
- [3] W. Li, H. El-Askary, M. A. Qurban, J. Li, K. P. Manikandan, and T. Piechota, "Using multi-indices approach to quantify mangrove changes over the Western Arabian Gulf along Saudi Arabia coast," *Ecol. Indic.*, vol. 102, pp. 734–745, Jul. 2019, doi: 10.1016/j.ecolind.2019.03.047.
- [4] W. Li *et al.*, "An Assessment of the Hydrological Trends Using Synergistic Approaches of Remote Sensing and Model Evaluations over Global Arid and Semi-Arid Regions," *Remote Sens.*, vol. 12, no. 23, Art. no. 23, Dec. 2020, doi: 10.3390/rs12233973.
- [5] R. H. Maneja *et al.*, "Long-term NDVI and recent vegetation cover profiles of major offshore island nesting sites of sea turtles in Saudi waters of the northern Arabian Gulf," *Ecol. Indic.*, vol. 117, p. 106612, Oct. 2020, doi: 10.1016/j.ecolind.2020.106612.
- [6] W. Li *et al.*, "Investigating Decadal Changes of Multiple Hydrological Products and Land-Cover Changes in the Mediterranean Region for 2009–2018," *Earth Syst. Environ.*, vol. 5, no. 2, pp. 285–302, Jun. 2021, doi: 10.1007/s41748-021-00213-w.
- [7] W. Li, H. M. El-Askary, M. Qurban, M. Allali, and K. P. Manikandan, "On the Drying Trends Over the MENA Countries Using Harmonic Analysis of the Enhanced Vegetation Index," in *Advances in Remote Sensing and Geo Informatics Applications*, H. M. El-Askary, S. Lee, E. Heggy, and B. Pradhan, Eds., in *Advances in Science, Technology & Innovation*. Cham: Springer International Publishing, 2019, pp. 243–245. doi: 10.1007/978-3-030-01440-7_57.
- [8] B. Qiu, W. Li, Z. Tang, C. Chen, and W. Qi, "Mapping paddy rice areas based on vegetation phenology and surface moisture conditions," *Ecol. Indic.*, vol. 56, pp. 79–86, Sep. 2015, doi: 10.1016/j.ecolind.2015.03.039.
- [9] R. Ni *et al.*, "An enhanced pixel-based phenological feature for accurate paddy rice mapping with Sentinel-2 imagery in Google Earth Engine," *ISPRS J. Photogramm. Remote Sens.*, vol. 178, pp. 282–296, Aug. 2021, doi: 10.1016/j.isprsjprs.2021.06.018.
- [10] W. Li, D. Li, and Z. N. Fang, "Intercomparison of Automated Near-Real-Time Flood Mapping Algorithms Using Satellite Data and DEM-Based Methods: A Case Study of 2022 Madagascar Flood," *Hydrology*, vol. 10, no. 1, p. 17, Jan. 2023, doi: 10.3390/hydrology10010017.
- [11] N. Karimi and M. R. Taban, "A convex variational method for super resolution of SAR image with speckle noise," *Signal Process. Image Commun.*, vol. 90, p. 116061, Jan. 2021, doi: 10.1016/j.image.2020.116061.
- [12] R. Chastain, I. Housman, J. Goldstein, M. Finco, and K. Tenneson, "Empirical cross sensor comparison of Sentinel-2A and 2B MSI, Landsat-8 OLI, and Landsat-7 ETM+ top of atmosphere spectral characteristics over the conterminous United States," *Remote Sens. Environ.*, vol. 221, pp. 274–285, Feb. 2019, doi: 10.1016/j.rse.2018.11.012.
- [13] E. Çolak, M. Chandra, and F. Sunar, "THE USE OF SENTINEL 1/2 VEGETATION INDEXES WITH GEE TIME SERIES DATA IN DETECTING LAND COVER CHANGES IN THE SINOP NUCLEAR POWER PLANT CONSTRUCTION SITE," *Int. Arch. Photogramm. Remote Sens. Spat. Inf. Sci.*, vol. XLIII-B3-2021, pp. 701–706, Jun. 2021, doi: 10.5194/isprs-archives-XLIII-B3-2021-701-2021.
- [14] "Statewide Crop Mapping - California Natural Resources Agency Open Data." <https://data.cnra.ca.gov/dataset/statewide-crop-mapping> (accessed Jan. 20, 2023).
- [15] G. Yang *et al.*, "AGTOC: A novel approach to winter wheat mapping by automatic generation of training samples and one-class classification on Google Earth Engine," *Int. J. Appl. Earth Obs. Geoinformation*, vol. 102, p. 102446, Oct. 2021, doi: 10.1016/j.jag.2021.102446.